Self-consistent hybrid approach for complex systems: Application to the spin-boson model with Debye spectral density

Michael Thoss,[a] Haobin Wang, and William H. Miller
Department of Chemistry and Kenneth S. Pitzer Center for Theoretical Chemistry, University of California, Berkeley, California 94720-1460 and Chemical Sciences Division, Lawrence Berkeley National Laboratory, Berkeley, California 94720

(Received 28 February 2001; accepted 23 May 2001)

The self-consistent hybrid approach [H. Wang, M. Thoss, and W. H. Miller, J. Chem. Phys. **115**, 2979 (2001), preceding paper] is applied to the spin-boson problem with Debye spectral density as a model for electron-transfer reactions in a solvent exhibiting Debye dielectric relaxation. The population dynamics of the donor and acceptor states in this system is studied for a broad range of parameters, including the adiabatic (slow bath), nonadiabatic (fast bath), as well as the intermediate regime. Based on illustrative examples we discuss the transition from damped coherent dynamics to purely incoherent decay. Using the numerically exact results of the self-consistent hybrid approach as a benchmark, several approximate theories that have been widely used to describe the dynamics in the spin-boson model are tested: the noninteracting blip approximation, the Bloch–Redfield theory, the Smoluchowski-equation treatment of the reaction coordinate (Zusman equations), and the classical path approach (Ehrenfest model). The parameter range where the different methods are applicable are discussed in some detail. © *2001 American Institute of Physics.*
[DOI: 10.1063/1.1385562]

I. INTRODUCTION

Dissipative processes are a common phenomenon in the dynamics of complex systems in physics and chemistry.[1] The spin-boson model, a two-level system interacting linearly with a harmonic bath, is one of the best studied examples describing dissipative dynamics.[1,2] It has been applied to a variety of different problems in physics and chemistry, e.g., hydrogen tunneling in condensed media[3,4] or the description of macroscopic quantum coherence[5] and many others discussed in Ref. 1. In chemical physics it provides a model for electron transfer reactions in solution, protein complexes, or other condensed phase environments.[6–8]

There have been extensive studies on the dynamics of the spin-boson model.[2,6–32] While many of these are based on approximations that restrict the applicability to certain parameter regimes, there exist a few numerically exact treatments[10,14–18,24] based on the Feynman path-integral approach. These methods take advantage of the fact that for the spin-boson model the bath is harmonic and can be integrated out analytically, giving the Feynman–Vernon influence functional.[33,34] For situations where the memory effects implicit in the influence functional are only important on a short time scale (i.e., the bath correlation decays fast enough), efficient path integral calculations can be carried out. Otherwise, further approximations/improvements need to be adopted.[28,31]

A quite different approach, which was proposed recently by one of us,[32] is to solve the time-dependent Schrödinger equation for all the degrees of freedom (DoF), i.e., the two-level ''system'' plus the ''bath,'' using a basis-set method in a multiconfiguration time-dependent Hartree (MCTDH) context.[35–37] In this way, numerically exact results for the spin-boson model can be obtained via a standard type of variational calculation, which has been proven to be as efficient as the path integral method for the spin-boson model. Furthermore, in contrast to the path-integral influence-functional approach, this method is by construction not limited to a harmonic bath or linear coupling between the system and the bath.

Most of the approximate methods that have been applied to study the dynamics of the spin-boson model are based on some kind of perturbation theory. They differ primarily in the specific part of the spin-boson Hamiltonian that is treated perturbatively. Examples of these methods include the noninteracting-blip approximation[2,9] (NIBA) and different variants of Redfield theory or master-equation approaches.[6,7,12,20,30,27]

Besides these perturbation-theory methods, several ''mixed quantum-classical'' approaches have been applied to the spin-boson model,[19,31,38,39] most notably the classical-path approach[40–46] (or Ehrenfest model) (which is closely related to the linearized semiclassical initial value representation/classical Wigner method[25,26]) and the surface-hopping method.[47–53] In these methods the electronic (two-level) system is treated quantum mechanically whereas the dynamics of the bath degrees of freedom (DoF) is described by classical mechanics. They differ in the way how the quantum and the classical subsystems are coupled. Treating all bath DoF classically, these methods usually provide good results for a slow bath (i.e., the characteristic frequency of the bath ω_c is smaller than the electronic coupling Δ) and/or high temperature ($\omega_c \ll k_B T$). If neither of these conditions is

[a]Present address: Theoretische Chemie, Technische Universität München, D-85747 Garching, Germany.

fulfilled these methods fail, for example, they cannot describe the relaxation dynamics correctly. This failure is related to the fact that a part of the bath (typically the high frequency modes), which would require a quantum mechanical treatment, is treated classically.[29,31,39]

Golosov, Friesner, and Pechukas have recently proposed a method which circumvents this problem by expressing the overall bath spectral density as a sum of two spectral densities. Overlapping with each other, one spectral density has a low characteristic frequency, whereas another has a higher one. The latter was combined with the electronic two-state system to form a composite ''quantum subsystem,'' and the former is classified as ''classical subsystem.'' [31] Approximate theories that are appropriate in these two physical limits are then combined to treat the overall system, namely, the memory equation approach (approximation to the path integral method) for the ''quantum subsystem'' and classical mechanics for the ''classical subsystem.''

In a preceding paper,[54] henceforth referred to as paper I, we have proposed a self-consistent hybrid approach to accurately simulate quantum dynamics for complex systems. The first step of the method is similar in spirit to that of Golosov *et al.*[31] and many other hybrid approaches, i.e., the overall system is divided into a ''core'' and a ''reservoir.'' The dynamics of the core is treated by a high level quantum mechanical method, whereas that of the reservoir is treated at a more approximate level of theory. As has been discussed in detail in paper I, the particular choice of the method for core and reservoir depends on the physics of the problem under consideration. For applications to the spin-boson model at finite temperatures in this paper, we mainly use classical mechanics (with the correct initial phase space distribution) to describe the reservoir. Accordingly, the core comprises the two electronic states and in most cases the high frequency modes of the bath, and the reservoir contains the remaining bath modes. The core is treated using the MCTDH method (which allows one to treat a rather large system quantum mechanically[55,56]). The coupling between the classical and quantum degrees of freedom is accomplished as in the classical path method, i.e., the classical trajectories enter the dynamics of the quantum system via a parametric dependence of the Hamiltonian, and the wave function of the quantum part affects the classical trajectories through the average force.

The major difference between our method and other previously applied hybrid approaches (including the classical path method) is that we cast the core–reservoir separation, an often intuitive but otherwise rather arbitrary choice, into a self-consistent convergence procedure. Not only the electronic degree of freedom is treated quantum mechanically, but also the ''quantum'' part of the bath. Furthermore, the part of the bath which is included in the core is increased systematically until convergence is reached. Therefore, very similar to a usual variational calculation, this hybrid approach adopts an iterative procedure to achieve the final convergence: besides variational parameters that appear in a regular basis set MCTDH calculation (number of basis functions, number of configurations, etc.), the core–reservoir partition is also varied. By definition, true quantum mechanical results are obtained when all the degrees of freedom are included in the core. In practice, however, converged results are often obtained well before such a rigorous level of theory.[54] Thus, this approach is, in principle, a numerically exact method and can ''automatically'' tune the portion of the overall system that is treated at a more approximate level of theory. Different from the approach of Golosov *et al.*, this method is not based on the influence-functional approach and, therefore, can be applied to a nonlinear bath as well. As was demonstrated in paper I, it is, furthermore, not restricted to a low-dimensional (e.g., two or three level) electronic system.

In paper I we have introduced the method and demonstrated the performance for a spin-boson system with Ohmic spectral density as well as for the decay of electronic resonances in presence of a vibrational bath. In the present paper we will apply this method to a spin-boson model with Debye spectral density as a model for electron transfer reactions in a Debye solvent. The purpose of this study is twofold: First, the new method allows us to study this model in a rather broad parameter range (varying the coupling strength η, the characteristic frequency of the bath ω_c, and the temperature T). Second, using the hybrid approach results as a benchmark, we will test several approximate methods which have been extensively used for this model in the recent years: the noninteracting-blip approximation, Bloch–Redfield theory, the master-equation/Smoluchowski-equation treatment of the reaction coordinate, as well as the classical-path method.

II. SUMMARY OF THEORY

A. Hamiltonian and observables of interest

The spin-boson Hamiltonian,

$$H = H_S + H_{SB} + H_B \tag{2.1}$$

describes an electronic two-level system,

$$H_S = \begin{pmatrix} \epsilon & \Delta \\ \Delta & -\epsilon \end{pmatrix} = \epsilon\sigma_z + \Delta\sigma_x, \tag{2.2}$$

characterized by the energy bias ϵ and the coupling Δ of the two electronic states, interacting with a bath of harmonic oscillators,

$$H_B = \sum_j \frac{1}{2}(p_j^2 + \omega_j^2 x_j^2), \tag{2.3}$$

through a bilinear coupling,

$$H_{SB} = \sigma_z \sum_j c_j x_j. \tag{2.4}$$

Here, σ_x and σ_z are the Pauli matrices, x_j and p_j denote the coordinate and momentum of the jth bath mode with frequency ω_j, respectively. (We use mass scaled coordinates and units with $\hbar = 1$ throughout the paper.) In the context of electron-transfer theory the two electronic states correspond to the donor and acceptor state, respectively.

The bath is characterized by its spectral density,[1,2]

$$J(\omega) = \frac{\pi}{2} \sum_j \frac{c_j^2}{\omega_j} \delta(\omega - \omega_j). \tag{2.5}$$

In the present paper we consider a bath with spectral density in the so-called Debye form,[8,26,57–59]

$$J(\omega)=\frac{\eta\,\omega_c\,\omega}{\omega_c^2+\omega^2}. \tag{2.6}$$

This spectral density is linear (Ohmic) for small frequencies but has a Lorentzian cutoff. (It is sometimes also referred to as an Ohmic spectral density with Drude cutoff.[1]) It describes a solvent exhibiting Debye dielectric relaxation. The two parameters which characterize the spectral density, the characteristic bath frequency ω_c and the coupling strength η, are related to other physical quantities: $1/\omega_c=\tau_L$ is the longitudinal relaxation time of the solvent and $E_r=2\eta$ is the reorganization energy in electron-transfer theory. As was discussed in Ref. 26, the Debye spectral density spans a much broader frequency range than the usual Ohmic case ($J_O=(\pi/2)\,\alpha\omega e^{-\omega/\omega_c}$) and thus represents a greater challenge to numerical simulations.

To study the dynamics of the spin-boson model we will primarily focus on the population difference of the two electronic states,

$$\begin{aligned}P(t)&=P_1(t)-P_2(t)\\&=\langle\sigma_z(t)\rangle=\mathrm{tr}\{\rho_B|1\rangle\langle 1|e^{iHt}\sigma_z e^{-iHt}\}.\end{aligned} \tag{2.7}$$

In Eq. (2.7) we have assumed a factorized initial state: the electronic system is initially in state $|1\rangle$ (the donor state) and the bath is in thermal equilibrium described by the Boltzmann operator,

$$\rho_B=\frac{e^{-\beta(H_B-y_0\Sigma_j c_j x_j)}}{Z_B},\quad Z_B=\mathrm{tr}_B(e^{-\beta(H_B-y_0\Sigma_j c_j x_j)}). \tag{2.8}$$

This initial condition corresponds, for example, to a photoinduced electron-transfer process, where photoexcitation takes place from a lower-lying electronic state to the donor state. The dimensionless parameter y_0 determines the average position of the initial state, which for a photoinduced electron-transfer process is given by the equilibrium geometry of the lower-lying electronic state from which photoexcitation takes place.[20,23] A value of $y_0=-1$, for example, corresponds to an initial state where the nuclear degrees of freedom are in equilibrium at the donor state. A value of $y_0=0$, on the other hand, describes a nonequilibrium initial state centered around $x_j=0$.

We will also present some results for electron-transfer rates, which can be obtained from $P(t)$ if the population dynamics exhibits exponential decay. In particular, we will compare results obtained from numerically exact and approximate dynamical approaches with results obtained from commonly used rate formulas such as, for example, the Golden Rule rate.

B. Numerically exact self-consistent hybrid approach

The hybrid method we have used to simulate the dynamics of the spin-boson system was in detail described in paper I. Briefly, after a discretization of the bath, which (depending on the specific parameters under consideration and the timescale of interest) usually requires between 50 and a few hundred modes, the overall system is partitioned into a ''core'' and a ''reservoir.'' The former is treated via a high level quantum mechanical method and the latter is treated via a more approximate method. For the applications in this paper we have used the MCTDH method[35–37] for the core (which allows us to treat a rather large system quantum mechanically) and classical mechanics for the reservoir. Accordingly, the core comprises the two electronic states as well as vibrational modes with frequencies $\omega>\omega_q$. The reservoir comprises the remaining low frequency modes ($\omega<\omega_q$). As described in detail in paper I, a sensible initial guess for ω_q can be obtained using a thermal criterion. Test calculations are then carried out and the number of modes included in the core (as well as other variational parameters) is increased systematically until convergence (usually to within 10% relative error) is reached. If all the bath modes were treated classically (i.e., the core comprised only the electronic two-state system) this method would be equivalent to the classical path (Ehrenfest) method. But because the calculation is converged with respect to the number of bath modes included in the quantum propagation, the results are numerically exact.

C. Approximate methods

A variety of different approximate methods have been applied to the spin-boson model. Most of these methods are either based on a perturbative treatment of a part of the Hamiltonian or use classical concepts to treat the dynamics of the bath. It is one intention of this paper to test some of these more approximate methods with the results of our simulation. For this purpose, we have chosen four methods which have been used extensively in the recent years: the noninteracting-blip approximation (NIBA), the Bloch–Redfield equation (BRE) approach, the master-equation/Smoluchowski-equation treatment of the reaction coordinate, and the classical-path method. To facilitate the discussion of the results and to keep the paper self-contained we will give a brief review of these methods in this subsection.

1. Noninteracting-blip approximation

The NIBA was originally derived by Leggett and coworkers using the path-integral influence-functional method.[2] Later, Aslagul *et al.* have shown that it can also be obtained using standard reduced density matrix perturbation theory.[9] Thereby, the (bath-dressed) electronic coupling is the part of the Hamiltonian which is treated within perturbation theory. Within the NIBA the population difference between the two electronic states is given by the solution of the integro-differential equation,

$$\frac{\mathrm{d}}{\mathrm{d}t}P(t)=-\int_0^t \mathrm{d}\tau\,(K_+(t,\tau)P(\tau)+K_-(t,\tau)). \tag{2.9}$$

Here, the two kernels are defined by

$$\begin{aligned}K_+(t,\tau)=(2\Delta)^2\cos(Q''(t-\tau))\cos[&2\epsilon(t-\tau)\\&+(1+y_0)(Q''(t)-Q''(\tau))]e^{-Q'(t-\tau)},\end{aligned} \tag{2.10a}$$

$$K_-(t,\tau)=(2\Delta)^2\sin(Q''(t-\tau))\sin[2\epsilon(t-\tau)+(1+y_0)(Q''(t)-Q''(\tau))]e^{-Q'(t-\tau)}, \tag{2.10b}$$

with

$$Q(\tau)=Q'(\tau)+iQ''(\tau)=\frac{4}{\pi}\int \mathrm{d}\omega\,\frac{J(\omega)}{\omega^2}[\coth(\beta\omega/2)(1-\cos(\omega\tau))+i\sin(\omega\tau)]. \tag{2.11}$$

As was discussed above, the parameter y_0 contains the information on the average position of the initial state of the bath.[20,23] Analytical investigations[1,2] as well as comparisons with results from path-integral calculations[15–17,31,60] (for Ohmic spectral densities) have shown that, in general, NIBA is a rather good approximation for nonadiabatic electron transfer (i.e., weak electronic coupling $\Delta/\omega_c \ll 1$), in particular for systems without electronic bias ($\epsilon=0$). It is also known that NIBA breaks down in biased systems ($\epsilon\neq 0$) for low temperature and weak coupling to the bath, for example, predicting a qualitatively incorrect asymptotic state in this parameter regime. While these limits of validity of NIBA have been investigated by several workers for an Ohmic spectral density, in this paper we will systematically study the quality of the NIBA for a bath with Debye spectral density.

2. Bloch–Redfield equation

While NIBA treats the (bath-dressed) electronic coupling perturbatively, a quite different approximation is obtained by treating the system–bath coupling within perturbation theory. In the simplest case H_{SB} is treated perturbatively resulting in a master equation for the reduced density matrix of the electronic two-level system.[2,9,61–63] If only perturbation theory (but no Markovian approximation) is used, the corresponding equations read

$$\frac{\mathrm{d}}{\mathrm{d}t}\langle\sigma_z(t)\rangle=2\Delta\langle\sigma_y(t)\rangle, \tag{2.12a}$$

$$\frac{\mathrm{d}}{\mathrm{d}t}\langle\sigma_x(t)\rangle=-2\epsilon\langle\sigma_y(t)\rangle-\int_0^t\mathrm{d}s\,\Gamma_x(s)-\int_0^t\mathrm{d}s[\Gamma_{xx}(s)\langle\sigma_x(t-s)\rangle+\Gamma_{xy}(s)\langle\sigma_y(t-s)\rangle], \tag{2.12b}$$

$$\frac{\mathrm{d}}{\mathrm{d}t}\langle\sigma_y(t)\rangle=2\epsilon\langle\sigma_x(t)\rangle-2\Delta\langle\sigma_z(t)\rangle-\int_0^t\mathrm{d}s\,\Gamma_y(s)-\int_0^t\mathrm{d}s[\Gamma_{yy}(s)\langle\sigma_y(t-s)\rangle+\Gamma_{yx}(s)\langle\sigma_x(t-s)\rangle]. \tag{2.12c}$$

The kernels for these integro-differential equations are given by

$$\Gamma_x(t)=\frac{\Delta}{\sqrt{\Delta^2+\epsilon^2}}\sin(2\sqrt{\Delta^2+\epsilon^2}t)M''(t), \tag{2.13a}$$

$$\Gamma_y(t)=\frac{\epsilon\Delta}{\Delta^2+\epsilon^2}(1-\cos(2\sqrt{\Delta^2+\epsilon^2}t))M''(t), \tag{2.13b}$$

$$\Gamma_{xx}(t)=\cos(2\sqrt{\Delta^2+\epsilon^2}t)M'(t), \tag{2.13c}$$

$$\Gamma_{yy}(t)=\frac{\Delta^2+\epsilon^2\cos(2\sqrt{\Delta^2+\epsilon^2}t)}{\Delta^2+\epsilon^2}M'(t), \tag{2.13d}$$

$$\Gamma_{xy}(t)=-\Gamma_{yx}(t)=-\frac{\epsilon}{\sqrt{\Delta^2+\epsilon^2}}\sin(2\sqrt{\Delta^2+\epsilon^2}t)M'(t), \tag{2.13e}$$

with

$$M(t)=M'(t)+iM''(t)=\frac{4}{\pi}\int\mathrm{d}\omega J(\omega)[\coth(\beta\omega/2)\cos(\omega\tau)+i\sin(\omega\tau)]. \tag{2.14}$$

The non-Markovian master equation (2.12) is supposed to give good results if the system–bath coupling is weak, i.e., if the dimensionless coupling parameter $\alpha=2\eta/\omega_c\pi$ is small.

A simpler, Markovian master equation with time-dependent rates can be obtained by relating the expectation values $\langle\sigma_{x/y/z}(t-s)\rangle$ to their values at time t, thereby neglecting the coupling to bath. In this way one obtains the following set of equations:[9,63]

$$\frac{\mathrm{d}}{\mathrm{d}t}\langle\sigma_z(t)\rangle=2\Delta\langle\sigma_y(t)\rangle, \tag{2.15a}$$

$$\frac{\mathrm{d}}{\mathrm{d}t}\langle\sigma_x(t)\rangle=-2\epsilon\langle\sigma_y(t)\rangle-\tilde{\Gamma}_x(t)-\tilde{\Gamma}_{xx}(t)\langle\sigma_x(t)\rangle-\tilde{\Gamma}_{xz}(t)\langle\sigma_z(t)\rangle, \tag{2.15b}$$

$$\frac{\mathrm{d}}{\mathrm{d}t}\langle\sigma_y(t)\rangle=2\epsilon\langle\sigma_x(t)\rangle-2\Delta\langle\sigma_z(t)\rangle-\tilde{\Gamma}_y(t)-\tilde{\Gamma}_{yy}(t)\langle\sigma_y(t)\rangle-\tilde{\Gamma}_{yz}(t)\langle\sigma_z(t)\rangle, \tag{2.15c}$$

with the time-dependent rates,

$$\tilde{\Gamma}_x(t)=\int_0^t\mathrm{d}s\,\Gamma_x(s), \tag{2.16a}$$

$$\tilde{\Gamma}_y(t)=\int_0^t\mathrm{d}s\,\Gamma_y(s), \tag{2.16b}$$

$$\tilde{\Gamma}_{yy}(t)=\tilde{\Gamma}_{xx}(t)=\int_0^t\mathrm{d}s\,\frac{\epsilon^2+\Delta^2\cos(2\sqrt{\Delta^2+\epsilon^2}s)}{\Delta^2+\epsilon^2}M'(s), \tag{2.16c}$$

$$\tilde{\Gamma}_{xz}(t)=-\frac{\epsilon\Delta}{\Delta^2+\epsilon^2}\int_0^t\mathrm{d}s(1-\cos(2\sqrt{\Delta^2+\epsilon^2}s))M'(s), \tag{2.16d}$$

$$\tilde{\Gamma}_{yz}(t)=\frac{\Delta}{\sqrt{\Delta^2+\epsilon^2}}\int_0^t \mathrm{d}s\,\sin(2\sqrt{\Delta^2+\epsilon^2}s)M'(s). \tag{2.16e}$$

For times long compared to the decay time of the bath correlation function (i.e., $\omega_c t\gg 1$) the rates (2.16) approach their stationary value and then equations (2.15) are equivalent to the Bloch or Redfield equation. We will therefore refer to Eqs. (2.12) and (2.15) as non-Markovian and Markovian Bloch–Redfield equations (BRE), respectively.

3. Master-equation/Smoluchowski-equation treatment of the reaction coordinate

An improved approximation can be obtained by including one (or several) reaction mode(s) into the system and treating the coupling to the rest of the bath (the ''secondary'' bath) perturbatively.[6,7,12,27,64–68] This method can be derived using the reaction-coordinate representation of the spin-boson Hamiltonian[7] which is given by

$$H=H_S+H_{SR}+H_R+H_{RB}+\tilde{H}_B, \tag{2.17}$$

with

$$H_R=\tfrac{1}{2}(p_y^2+\Omega^2 y^2), \tag{2.18a}$$

$$H_{SR}=\kappa y\sigma_z, \tag{2.18b}$$

$$H_{RB}+\tilde{H}_B=\frac{1}{2}\sum_\alpha\left[\tilde{p}_\alpha^2+\tilde{\omega}_\alpha^2\left(\tilde{x}_\alpha-\frac{\tilde{c}_\alpha y}{\tilde{\omega}_\alpha^2}\right)^2\right]. \tag{2.18c}$$

Here, y denotes the reaction coordinate with corresponding momentum p_y and frequency Ω, and κ is the coupling strength between the reaction coordinate and the electronic system. These quantities are related to the spin-boson Hamiltonian by the following identities:

$$\kappa y=\sum_j c_j x_j, \tag{2.19a}$$

$$\kappa=\sqrt{\sum_j c_j^2}, \tag{2.19b}$$

$$\Omega^2=\kappa^2\left(\sum_j c_j^2/\omega_j^2\right)^{-1}. \tag{2.19c}$$

In Eq. (2.18), the coordinates and momenta of the secondary bath, as well as their coupling constants and frequencies, are denoted with a tilde. The original representation of the spin-boson Hamiltonian, i.e., Eqs. (2.1)–(2.4), can be obtained from the reaction coordinate representation by a normal mode transformation of $H_R+H_{RB}+\tilde{H}_B$.

Defining the spectral density for the coupling of the reaction coordinate to the secondary bath as

$$\tilde{J}(\omega)=\frac{\pi}{2}\sum_\alpha\frac{\tilde{c}_\alpha^2}{\tilde{\omega}_\alpha}\delta(\omega-\tilde{\omega}_\alpha), \tag{2.20}$$

the formal relation to the spin-boson spectral density is given by[7,69]

$$J(\omega)=\frac{\kappa^2\tilde{J}(\omega)}{\left[\omega^2-\Omega^2-\frac{2}{\pi}\int_0^\infty \mathrm{d}s\,\frac{\omega^2\tilde{J}(s)}{s(\omega^2-s^2)}\right]^2+[\tilde{J}(\omega)]^2}, \tag{2.21}$$

where the integral in the denominator is to be understood as a principal value integral.

To describe a spin-boson model with Debye spectral density one cannot directly use the relations (2.19) to obtain the frequency and coupling strength of the reaction coordinate, because the first moment of the spectral density $\int \mathrm{d}\omega\,\omega J(\omega)$ (and also all higher moments) is divergent. Nevertheless, the mapping of the the spin-boson model with Debye spectral density to a reaction coordinate model is possible as a limiting case of a more general spectral density. To illustrate this mapping, let us consider a reaction coordinate Hamiltonian with Ohmic spectral density,

$$\tilde{J}(\omega)=\gamma\omega e^{-\omega/\Lambda}, \tag{2.22}$$

with exponential cutoff parameter Λ and coupling strength γ. Inserting this spectral density into Eq. (2.21) one obtains for a cutoff frequency Λ which is large compared to the reaction coordinate frequency Ω (i.e., $\Lambda/\Omega\gg 1$) the corresponding spin-boson spectral density,[7]

$$J(\omega)=\frac{\kappa^2\gamma\omega}{(\omega^2-\Omega^2)^2+(\gamma\omega)^2}=\frac{\kappa^2}{\gamma}\frac{\omega}{\omega^2+(\Omega^2/\gamma)^2+(\omega^2/\gamma)^2-2(\omega\Omega/\gamma)^2}. \tag{2.23}$$

The second line in Eq. (2.23) shows that in the limit of an overdamped reaction coordinate (i.e., $\Omega\ll\gamma/2$) this spectral density gives the Debye spectral density,

$$J(\omega)=\frac{\eta\omega_c\omega}{\omega_c^2+\omega^2}. \tag{2.24}$$

Thereby, ω_c is the decay rate of the overdamped reaction coordinate, i.e., $\omega_c=\Omega^2/\gamma$, and the overall coupling strength η is given by $\eta=\kappa^2/\Omega^2$. Therefore, the spin-boson Hamiltonian with Debye spectral density corresponds to a reaction coordinate Hamiltonian with Ohmic spectral density where the bath-cutoff frequency Λ and the coupling strength γ are large compared to the frequency Ω.

Defining the reduced density matrix for the electronic system and the reaction coordinate,

$$\rho(t)=\mathrm{tr}_{\tilde{B}}\{e^{-iHt}|1\rangle\rho_B\langle 1|e^{iHt}\}, \tag{2.25}$$

where $\mathrm{tr}_{\tilde{B}}$ denotes the trace over the secondary bath, and using perturbation theory with respect to the coupling between the reaction coordinate and the secondary bath (H_{RB}) as well as the Markov approximation, one can show that the dynamics of $\rho(t)$ is described by the master equation,[70]

$$\frac{\mathrm{d}}{\mathrm{d}t}\rho(t)=-i[H_S+H_{SR}+H_R,\rho(t)]-\frac{\gamma}{\beta}[y,[y,\rho(t)]]-\frac{i}{2}\gamma[y,\{p_y,\rho(t)\}]. \tag{2.26}$$

Here, $\{,\}$ denotes the anticommutator. This master equation, which was originally derived by Garg *et al.*[7] based on a similar treatment of Caldeira and Leggett,[71] is valid for high temperature, i.e., $\beta\sqrt{\Omega^2-\gamma^2/4}\ll 1$ in the underdamped case ($\Omega>\gamma/2$), and $\beta\Omega^2/\gamma\ll 1$ in the overdamped case ($\Omega<\gamma/2$), respectively.

As we have discussed above, the Debye spectral density corresponds to an overdamped reaction coordinate ($\gamma\gg\Omega$). In this limit it is possible (and advantageous) to eliminate the fast momentum of the reaction coordinate adiabatically.[72] This leads to the generalized Smoluchowski equation (GSE),

$$\frac{\partial}{\partial t}n_{11}(E,t)=\frac{\eta\omega_c}{\beta}\frac{\partial}{\partial E}\left[\frac{\beta}{\eta}(E+\eta)+\frac{\partial}{\partial E}\right]n_{11}+i\Delta(n_{12}-n_{21}), \tag{2.27a}$$

$$\frac{\partial}{\partial t}n_{22}(E,t)=\frac{\eta\omega_c}{\beta}\frac{\partial}{\partial E}\left[\frac{\beta}{\eta}(E-\eta)+\frac{\partial}{\partial E}\right]n_{22}-i\Delta(n_{12}-n_{21}), \tag{2.27b}$$

$$\frac{\partial}{\partial t}n_{12}(E,t)=\frac{\eta\omega_c}{\beta}\frac{\partial}{\partial E}\left[\frac{\beta}{\eta}E+\frac{\partial}{\partial E}\right]n_{12}-2i(\epsilon+E)n_{12}+i\Delta(n_{11}-n_{22}). \tag{2.27c}$$

Here, the generalized coordinate E (which represents the polarization energy[6]) is defined by $E=\kappa y$. The functions $n_{ij}(E,t)$ describe a probability distribution with respect to the coordinate E and a density matrix with respect to the electronic states. Accordingly, the population of the two electronic states is given by

$$P_i(t)=\int \mathrm{d}E\, n_{ii}(E,t). \tag{2.28}$$

The GSE (2.27) was introduced by Zusman[6] (it is, therefore, sometimes also referred to as the Zusman equation) and later derived by Garg *et al.*[7] as well as several other authors[12] using different methods. Cao and co-workers have analyzed its spectral structure recently.[27] Very recently, it was generalized to study electron-transfer reactions in strong time-dependent fields.[73] In the present paper we will systematically study the parameter range of its applicability.

III. RESULTS AND DISCUSSION

In this section we show results of simulations using the hybrid method for a broad range of the parameters of the spin-boson model. If the electronic coupling Δ is used as the unit of energy, the spin-boson model has four independent, dimensionless parameters: the electronic energy bias ϵ/Δ, the (inverse) temperature $\beta\Delta$, the coupling strength to the bath η/Δ, and the characteristic frequency of the bath ω_c/Δ. In the first part of this section we compare results obtained with the numerically exact hybrid method to results of the NIBA, the GSE, the BRE, as well as the classical path approach. For this purpose, we consider the adiabatic, nonadiabatic and intermediate parameter regimes separately. In the second part we discuss the coherent to incoherent transition of the population dynamics in the spin-boson model along the three parameter axis. Finally, in the third part, we will present some results for electron transfer rates.

A. Comparison with approximate methods

Depending on the ratio between electronic coupling and characteristic frequency of the bath Δ/ω_c, electron transfer reactions are commonly classified as adiabatic or nonadiabatic. In adiabatic reactions ($\Delta/\omega_c>1$), the characteristic timescale of the bath is slow compared to the electronic tunneling time. This case is realized, for example, in several mixed-valence compounds.[74–76] In nonadiabatic reactions ($\Delta/\omega_c<1$), on the other hand, the characteristic time scale of the bath is fast compared to the electronic tunneling dynamics. This case is typical for systems with a large separation between donor and acceptor, i.e. long-distance electron transfer.[77]

1. Adiabatic (slow bath) regime

Let us first focus on the adiabatic regime. In the limit of a very large adiabaticity parameter Δ/ω_c the nuclear degrees of freedom are quasistatic on the time scale of the electronic motion and the electronic population dynamics can be described by solving the Schrödinger equation for the bare electronic two-state system and averaging the result over the initial configuration of the nuclear degrees of freedom.[23,76,78] Therefore, in this limit the nuclear degrees of freedom effect the electronic dynamics only as a static disorder of the energy levels of the two electronic states. Here, we will concentrate on the more interesting regime of moderate adiabaticity with $\Delta/\omega_c=4$. Figure 1 depicts the results for a reasonably high temperature ($\beta\Delta=0.5$). The three panels illustrate the transition from a coherent, weakly-damped oscillation of the electronic population for small coupling [$\eta/\Delta=0.05$, panel (a), corresponding to $\alpha=0.127$] to an incoherent decay in the strong coupling regime [$\eta/\Delta=10$, panel (c), corresponding to $\alpha=12.732$]. It should be noted that the coherent oscillations in panels (a) and (b) represent an electronic coherence effect. As we have discussed above, the Debye spectral density corresponds to an overdamped reaction coordinate and, hence, cannot describe vibrational coherence.

For all three cases, the GSE results are in very good agreement with the numerically exact results of the self-consistent hybrid method. The NIBA result, on the other hand, has a phase-shift for weak coupling [panel (a)] and cannot even qualitatively describe the population dynamics in the medium to strong coupling regime. This is not too astonishing, because the derivation of the NIBA involves perturbation theory with respect to Δ/ω_c which is not a valid approximation in the parameter regime considered here.

Somewhat surprising at first sight is the failure of the BRE in the weak-coupling regime. Both the Markovian and non-Markovian BRE drastically underestimate the decay rate of the oscillations. The reason for this result can be understood from the perturbative approximation of the Bloch–Redfield theory. The first order rate which describes the de-

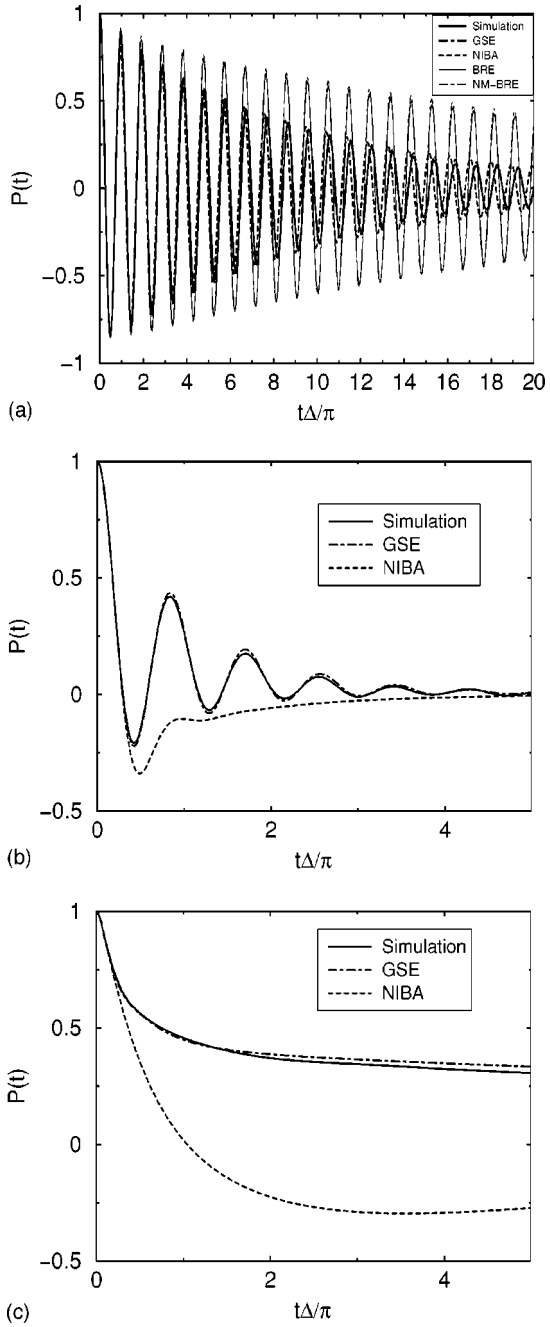

FIG. 1. Dynamics of the population difference of the two electronic states $P(t)$ in the adiabatic regime ($\Delta/\omega_c=4$) for $\beta\Delta=0.5$: (a) $\eta/\Delta=0.05$; (b) $\eta/\Delta=0.5$; (c) $\eta/\Delta=10$. Shown are the results of the hybrid approach simulation (full line), NIBA (dashed line), GSE (dashed–dotted line), and in panel (a) Markovian (thin full line) and non-Markovian (thin dashed–dotted line) BRE.

cay of the oscillation in the BRE is determined by the one phonon exchange rate. In the unbiased case ($\epsilon=0$) this rate is given by

$$\Gamma=\lim_{t\to\infty}\tilde{\Gamma}_{xx}(t)=2J(2\Delta)\coth(\beta\Delta), \tag{3.1}$$

and is proportional to the spectral density at the Rabi frequency (2Δ) of the two-level system. In the case considered here, the Rabi frequency is much larger than the characteristic frequency of the bath ($2\Delta/\omega_c=8$), resulting in a rather small first order rate Γ. Therefore, although the parameters considered in panel (a) are in the perturbative regime, one has to include higher order terms, i.e., multiphonon relaxation processes, to obtain a realistic description of the population decay.[79]

For the parameter regimes displayed in Fig. 1, i.e., a reasonably high temperature and a small characteristic frequency of the bath, it is generally believed that the bath can be treated classically. This is found from our self-consistent hybrid approach for not too strong electron–phonon couplings, Figs. 1(a) and 1(b). In these cases converged results are obtained if only the two electronic states are included in the core, i.e., the self-consistent hybrid method automatically ''tunes'' itself to the classical Ehrenfest model of the spin-boson problem.[29] Things become different for stronger electron–phonon coupling, Fig. 1(c), where 25% of the modes (starting from the high-frequency end of the spectral density) need to be included in the core and treated via the MCTDH method. The impact of treating these modes quantum mechanically is that the electronic population decays *more slowly* than that obtained from the classical Ehrenfest approach (where all modes are treated classically), somewhat counter-intuitive compared with the usual simple interpretation of ''tunneling'' contributions from the ''quantum modes.'' This suggests that quantum interference effects exist between the two electronic states and some of the high-frequency modes, which are captured well by the GSE as interactions between the two electronic states and the ''reaction coordinate.'' All other approximate theories examined in this paper fail to some extent in describing this effect.

Figure 2 shows the results obtained for an order of magnitude lower temperature. Due to the lower temperature the decay of the coherent oscillations for moderate coupling [panel (a)] is slower [compared to Fig. 1(b)] and even the result for strong coupling [panel (b)] shows remnants of coherence. For strong coupling it is also seen that $P(t)$ reaches a plateau after a certain time. This behavior signals the onset of localization, which is known to occur in the adiabatic regime for $E_r/\Delta>1$ in the zero temperature ($\beta\to\infty$) limit.[1] Because in the particular case considered here the temperature is small but finite, the plateau is only temporary and $P(t)$ will eventually decay to zero.

As to be expected from the discussion above, NIBA and BRE again fail to describe the dynamics. But in contrast to the high temperature case depicted in Fig. 1, also the GSE gives results which deviate significantly from the numerically exact results. In particular, the GSE cannot describe the damping of the oscillations correctly. This finding is related to the fact that the derivation of the GSE (2.27) involves a high temperature approximation ($\beta\omega_c<1$) which is not valid here. In the moderate coupling case [panel (a)], this shortcoming of the Smoluchowski approach can be circumvented to some extent by using full Redfield theory. In the strong coupling limit [panel (b)], however, it is presumably not possible to describe the dynamics with a perturbative method.

In the above cases, the self-consistent hybrid approach requires that 10% and 25% of the high-frequency modes be

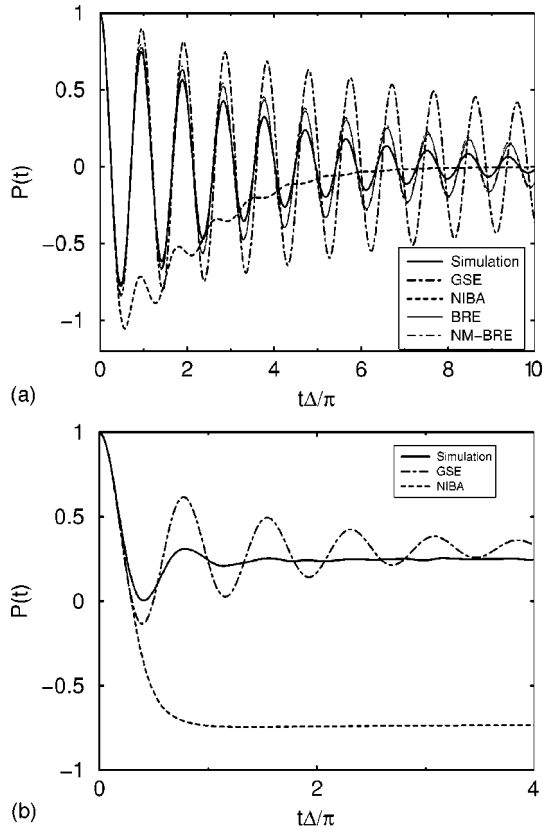

FIG. 2. Electronic population difference $P(t)$ in the adiabatic regime $(\Delta/\omega_c=4)$ for $\beta\Delta=5$: (a) $\eta/\Delta=0.5$; (b) $\eta/\Delta=5$. Shown are results of the hybrid approach simulation (full line), NIBA (dashed line), GSE (dashed–dotted line), and in panel (a) Markovian (thin full line) and non-Markovian (thin dashed–dotted line) BRE.

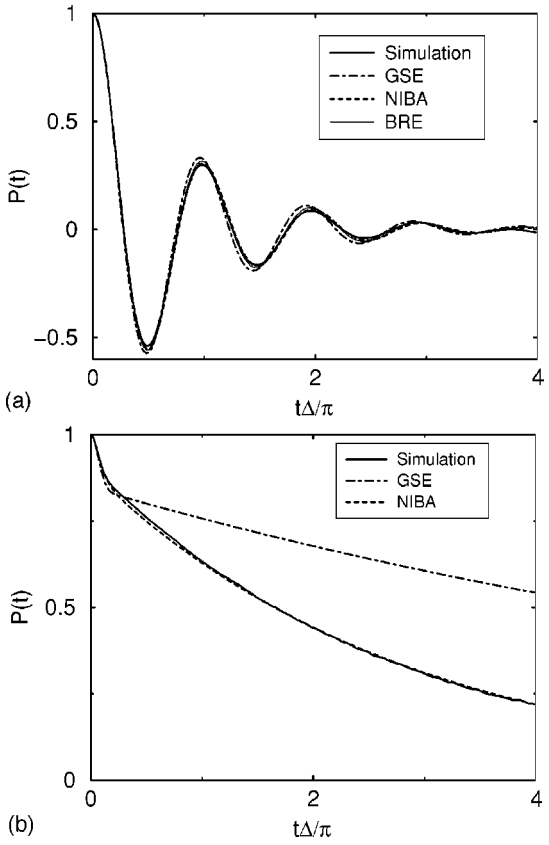

FIG. 3. Electronic population difference $P(t)$ in the nonadiabatic regime $(\Delta/\omega_c=0.2)$ for $\beta\Delta=0.5$: (a) $\eta/\Delta=0.5$; (b) $\eta/\Delta=10$. Shown are results of the hybrid approach simulation (full line), NIBA (dashed line), GSE (dashed–dotted line) and in panel (a) Markovian BRE (thin full line).

included in the core and treated via MCTDH, for Figs. 2(a) and 2(b), respectively. It is often expected that for the lower temperature case of Fig. 2, more (high-frequency) bath modes need to be treated quantum mechanically. However, somewhat to our surprise we found that the classical Ehrenfest approach provides an excellent approximation for weak electron–phonon coupling, Fig. 2(a), much better than any of the other approximate methods examined in this paper. For the stronger coupling case of Fig. 2(b), on the other hand, the classical Ehrenfest approach is no longer a good approximation. This finding, combined with the higher temperature results shown in Fig. 1, demonstrates that the classical Ehrenfest model is likely to work for adiabatic parameter regimes only when the electron–phonon coupling is not too large.

2. Nonadiabatic (fast bath) regime

We next consider the opposite regime, i.e. nonadiabatic electron transfer with $\Delta/\omega_c=0.2$. Figure 3 displays the results of the different methods for a temperature $\beta\Delta=0.5$. [It should be noted, that although this temperature is larger than the electronic coupling Δ it is smaller than the characteristic frequency of the bath $(\beta\omega_c=2.5)$.] As for the adiabatic case, a coherent to incoherent transition is observed when the coupling strength to the bath is increased from $\eta/\Delta=0.5$ [panel (a), corresponding to $\alpha=0.0637$] to $\eta/\Delta=10$ [panel (b), corresponding to $\alpha=1.273$].

NIBA is seen to be in excellent agreement with the results of the self-consistent hybrid method [20% and 50% of all bath modes are treated as quantum core modes for the converged results of panels (a) and (b), respectively] over the whole range of coupling strengths. The GSE, the BRE as well as the classical Ehrenfest model (not shown) can also reproduce the weak-coupling result [panel (a)] very well. For the BRE this is to be expected due to the small coupling strength. For the GSE this finding is somewhat surprising, because the assumption that the temperature is high compared to the characteristic frequency of the bath ω_c, which is usually invoked in the derivation of the GSE,[7] is not fulfilled here $(\beta\omega_c=2.5)$. For the same reason one would have expected a worse result from the classical Ehrenfest approach. The rationale of this is that if the electron–phonon coupling is sufficiently weak, most approximate theories are likely to work. If the coupling strength η is increased, the GSE and classical Ehrenfest approaches eventually break down. The result in Fig. 3(b), for example, demonstrates that for strong coupling the GSE significantly underestimates the long-time decay rate of $P(t)$.

Figure 4 displays the results for a temperature that is two orders of magnitude lower. Due to the low temperature, the damping rate of the oscillations is rather small. In this regime NIBA, as well as BRE, reproduce the simulation results quantitatively. The GSE, on the other hand, cannot describe the dynamics at all in this regime. Since the temperature is

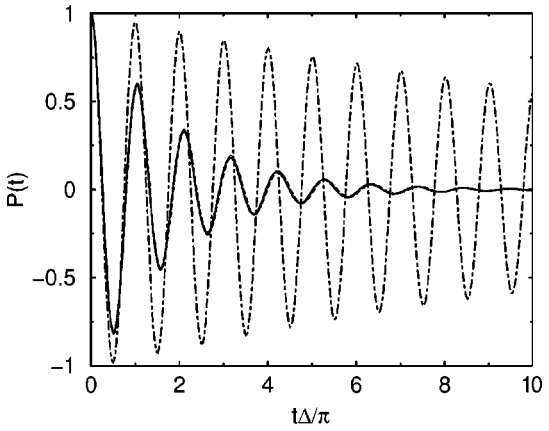

FIG. 4. Electronic population difference $P(t)$ in the nonadiabatic regime ($\Delta/\omega_c=0.2$) for $\beta\Delta=50$ and $\eta/\Delta=0.5$. Shown are results of the hybrid approach simulation (full line), NIBA (dashed line), GSE (dashed–dotted line), and Markovian BRE (thin full line).

very low here, most of the bath modes exhibit strong quantum mechanical character. As described in paper I, we therefore use a different strategy in the self-consistent hybrid approach: the *low*-frequency modes are put into the core and treated via the MCTDH method, and the *high*-frequency modes are put into the reservoir and treated via perturbation theory. For Fig. 4, convergence is achieved when 40% of the total bath modes are included in the core. Of course, the mixed quantum-classical strategy for the self-consistent hybrid approach still works, but is less efficient because most bath modes need to be included in the core.

3. Intermediate regime

Finally, we consider the intermediate regime with $\Delta/\omega_c=1$. In this regime neither Δ/ω_c nor ω_c/Δ can be treated as a small parameter and, therefore, NIBA as well as the classical path method are not expected to work well, and that is indeed what we have found. On the other hand, our numerical studies show that if the temperature is sufficiently high, and the coupling to the bath is not too strong, the GSE gives good results. For example, we found good agreement of the GSE results with those of the hybrid approach for $\beta\Delta\leqslant 0.5$ and $\eta/\Delta\leqslant 10$. In the low temperature regime, on the other hand, GSE is bound to fail. If the coupling to the bath is weak, BRE gives rather good results. Such a case is shown in Fig. 5(a). But if the coupling to the bath is moderate or strong, we found that none of the tested approximate methods can describe the dynamics reasonably well. Figure 5(b) displays the results of the different methods in this parameter regime. It is seen that after a short period of fast decay the system exhibits a transition to a much smaller decay rate. NIBA cannot describe this transition at all. The Smoluchowski equation, although capable of describing the bimodal decay qualitatively, overestimates the stabilization. It should also be noted that in both cases, the converged self-consistent hybrid calculation requires that more than 50% of the bath modes be included in the core and treated accurately, whereas the classical Ehrenfest approach provides quite poor results.

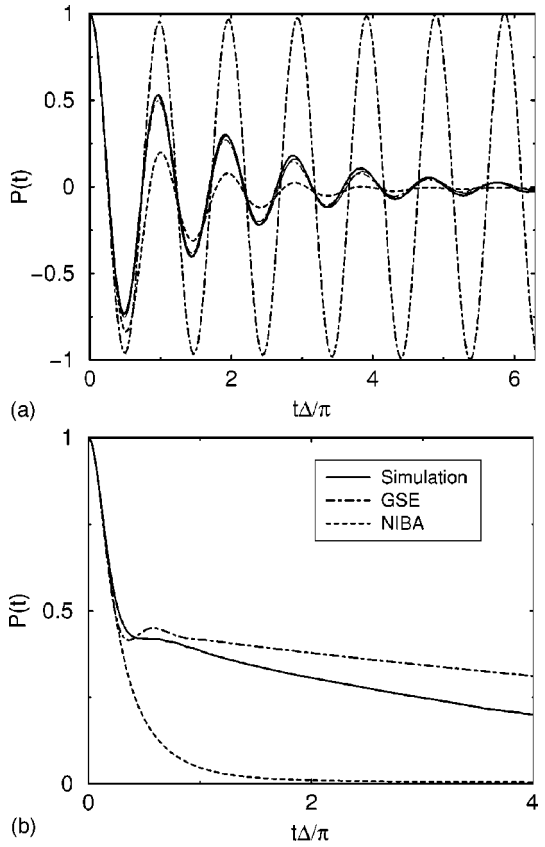

FIG. 5. Electronic population difference $P(t)$ in the intermediate regime ($\Delta/\omega_c=1$): (a) $\beta\Delta=50$, $\eta/\Delta=0.5$; (b) $\beta\Delta=1$, $\eta/\Delta=5$. Shown are results of the hybrid approach simulation (full line), NIBA (dashed line), GSE (dashed–dotted line), and in panel (a) Markovian (thin full line) and non-Markovian (thin dashed–dotted line) BRE.

4. Systems with electronic energy bias ($\epsilon\neq 0$)

So far we have only considered systems without electronic energy bias, i.e., $\epsilon=0$, corresponding to symmetrical electron-transfer reactions. In this subsection we will show some results for systems with an electronic bias. For this purpose we have chosen a value of $\epsilon/\Delta=1$. Generally speaking, most of the approximate methods become worse with inclusion of this energy bias (compared with the corresponding unbiased cases) and more caution must be taken in justifying the physical regimes to which they apply.

Figure 6 displays the results in the adiabatic, high-temperature regime for a moderate coupling strength. The main difference from the corresponding unbiased case [cf. Fig. 1(b)] is that the long-time limit of the population difference of the two electronic states is no longer zero. As to be expected, NIBA and BRE give qualitatively incorrect results in this parameter regime. Different from the unbiased case, however, the GSE also shows some deviations from the simulation results, in particular its long-time limit is lower. Further numerical simulations in the adiabatic regime for parameters corresponding to the unbiased cases depicted in Figs. 1 and 2 have revealed that these three approximate methods produce results that are in poorer agreement with the simulation (compared with the unbiased cases).

We next turn to the nonadiabatic regime. Figure 7 shows the results for small coupling and high temperature. As in the

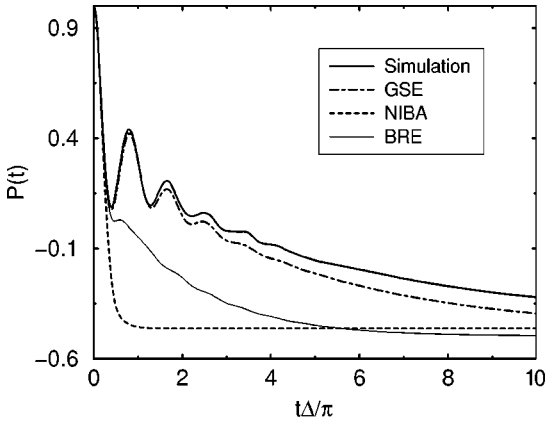

FIG. 6. Dynamics of the population difference of the two electronic states $P(t)$ in the adiabatic regime ($\Delta/\omega_c=4$) for $\beta\Delta=0.5$ with electronic energy bias $\epsilon/\Delta=1$ and coupling $\eta/\Delta=0.5$. Shown are the results of the hybrid approach simulation (full line), NIBA (dashed line), GSE (dashed–dotted line), and Markovian (thin full line) BRE.

corresponding unbiased case [cf. Fig. 3(a)], all approximate methods we have tested reproduce the dynamics qualitatively correctly. However, only BRE is able to describe the correct long-time limit; all other methods predict too low a value.

Figure 8 shows the results for a temperature two orders of magnitude lower. As to be expected, GSE is not a valid approximation in this very low temperature regime. In fact, it does not even preserve positivity any more. Furthermore, NIBA is seen to deviate (after a short time) and give an incorrect long-time limit. This failure of NIBA for systems with electronic energy bias in the low-temperature, weak-coupling regime is well-known (see, for example, Ref. 1). NIBA predicts the long-time limit,

$$P_{\mathrm{NIBA}}(t\to\infty)=-\tanh(\beta\epsilon), \tag{3.2}$$

which corresponds in the present case to a value of $P_{\mathrm{NIBA}}=0.9999$, whereas the physically correct value (in the weak coupling limit) is

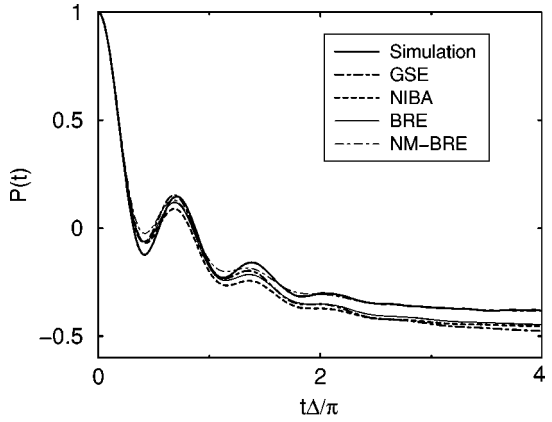

FIG. 7. Dynamics of the population difference of the two electronic states $P(t)$ in the nonadiabatic regime ($\Delta/\omega_c=0.2$) for $\beta\Delta=0.5$ with electronic energy bias $\epsilon/\Delta=1$ and coupling $\eta/\Delta=0.5$. Shown are the results of the hybrid approach simulation (full line), NIBA (dashed line), GSE (dashed–dotted line), and Markovian (thin full line), and non-Markovian (thin dashed–dotted line) BRE.

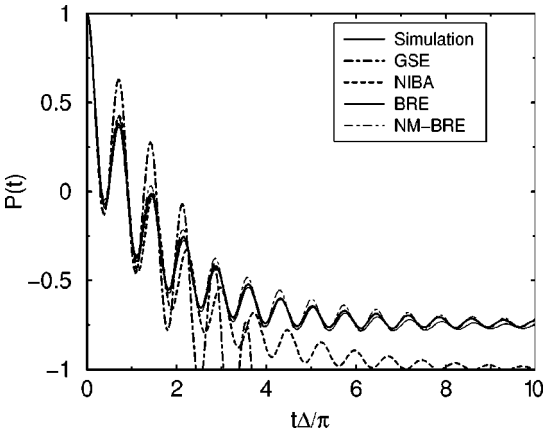

FIG. 8. Same as Fig. 7 but for lower temperature $\beta\Delta=50$.

$$P(t\to\infty)=-\frac{\epsilon}{\sqrt{\Delta_{\mathrm{eff}}^2+\epsilon^2}}\tanh(\beta\sqrt{\Delta_{\mathrm{eff}}^2+\epsilon^2}), \tag{3.3}$$

where Δ_{eff} denotes the ''bath-dressed'' electronic coupling,[1,30] corresponding to $P_\infty=-0.7288$. This latter value is in rather good agreement with the long-time limits of the simulation and the non-Markovian BRE. The Markovian BRE gives a slightly smaller value, demonstrating that although ω_c is already rather large there are still notable non-Markovian effects.

The inclusion of the electronic energy bias seems to have a major impact on the performance of the classical Ehrenfest approach. Similar to the above findings of NIBA and GSE, the classical Ehrenfest approach predicts an incorrect long time limit of the electronic population for nearly all the parameter regimes (except in the high temperature limit).[80] Thus, in order to describe nonsymmetric electron-transfer process with a hybrid approach, one needs to treat part of the bath quantum mechanically.

B. Coherent to incoherent transition

As was already mentioned briefly, the dynamics of the electronic population in the spin-boson model exhibits a transition from damped coherent oscillations to purely incoherent decay.[1,2] In the context of electron-transfer theory the study of this coherent to incoherent transition is of particular interest because it is closely related to the questions of occurrence, observability and quenching of quantum coherence effects in electron-transfer reactions which have been investigated recently in a variety of systems both experimentally and theoretically.[23,27,68,81–85] As will be discussed in more detail in Sec. III C, information on the coherent to incoherent transition is also important for a proper definition of electron-transfer rates.

Within the spin-boson model there are two sources of coherence: vibrational coherence, reflecting the coherent wave-packet dynamics of the reaction mode, and electronic coherence, reflecting the Rabi-oscillations of the bare two-level system. The model for a Debye solvent considered here corresponds to an overdamped reaction coordinate and, therefore, does not exhibit vibrational coherence. In this section we will study the quenching of electronic coherence as a

function of all three parameters of the unbiased spin-boson model. A similar study was recently carried out by Wang *et al*. using an approximate semiclassical method.[26] Here we base our discussion on the results of the numerically exact hybrid method.

1. Along the η-axis

This is the most obvious axis for observing the coherent to incoherent transition. The parameter η is a measure of the coupling strength to the bath (recall that the corresponding dimensionless coupling strength is given by $\alpha = 2\eta/\pi\omega_c$). Therefore, as η increases the energy exchange between the electronic two-level system and the bath becomes more efficient, and as a result the coherent motion of the two-level system is damped faster. This transition can be seen both in the adiabatic and nonadiabatic regime in Fig. 1 and Fig. 3, respectively. Whereas for a rather small value of $\eta/\Delta = 0.5$ [Fig. 1(b) and Fig. 3(a)] $P(t)$ exhibits damped coherent oscillations, all coherent features are quenched by the bath for strong coupling $\eta/\Delta = 10$ [Fig. 1(c) and Fig. 3(b)]. The precise value of η/Δ at which the transition occurs of course depends on the characteristic frequency of the bath and the temperature. For the adiabatic case depicted in Fig. 1, the transition occurs at $\eta/\Delta \approx 5$, and for the nonadiabatic case shown in Fig. 2 at $\eta/\Delta \approx 2$.

2. Along the T-axis

For fixed coupling strength η and characteristic frequency of the bath ω_c, the coherent to incoherent transition can be observed as the temperature T is increased. This is because for increasing temperature more bath states become energetically accessible and participate in the energy transfer which tends to destroy the coherent motion of the two-level system. The coherent to incoherent transition along the T-axis is of particular interest from an experimental point of view because, in contrast to η and ω_c, the temperature can be controlled more easily.

This low to high temperature coherent to incoherent transition is illustrated in Fig. 9. Panel (a) shows $P(t)$ in the adiabatic, moderate-coupling regime for different temperatures. It is seen that in this regime a rather high temperature ($\beta\Delta \approx 0.05$) is necessary to obtain a purely incoherent decay. In the nonadiabatic regime illustrated in panel (b), the transition occurs already at lower temperature ($\beta\Delta \approx 0.5$).

3. Along the ω_c-axis

While in many solid-state physics applications of the spin-boson model the nonadiabatic ($\Delta/\omega_c \ll 1$) regime is primarily of interest, in chemical physics, and in particular in the context of electron-transfer reactions, both the adiabatic and intermediate regime have many applications. Therefore, it is interesting to study the coherent to incoherent transition along the ω_c-axis. The physics behind this transition is that the bath has to be sufficiently fast in order to facilitate an incoherent decay of the electronic population.

To observe the coherent to incoherent transition along the ω_c-axis one has to choose a rather strong coupling and not too low a temperature. Figure 10 shows $P(t)$ in this parameter regime for different values of ω_c/Δ. For very small ω_c the bath is too slow to cause effective energy exchange and therefore $P(t)$ exhibits pronounced coherent oscillations. As ω_c increases, the bath becomes faster and thus the energy exchange between the two-level system and the bath becomes more efficient. Already at a rather small value of $\omega_c/\Delta = 0.25$, the dynamics of the electronic population is dominated by incoherent decay.

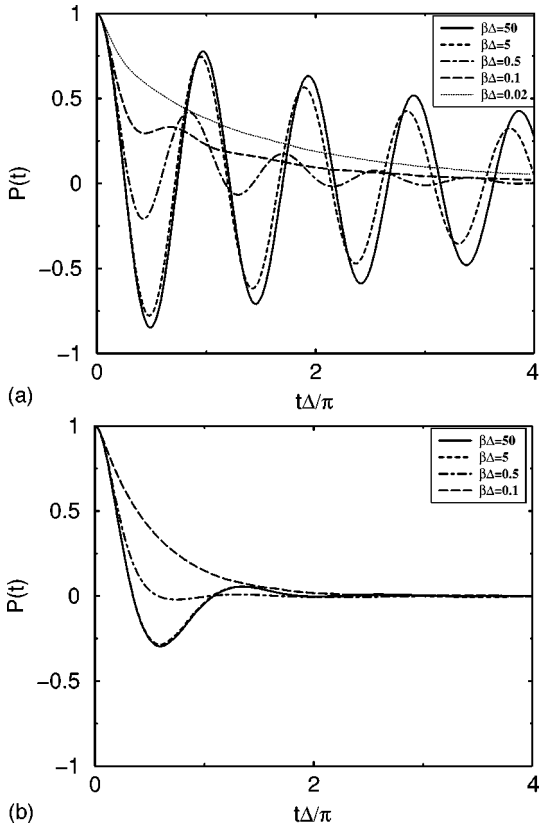

FIG. 9. Coherent to incoherent transition along the T-axis: (a) $\Delta/\omega_c = 4$, $\eta/\Delta = 0.5$; (b) $\Delta/\omega_c = 0.2$, $\eta/\Delta = 2$.

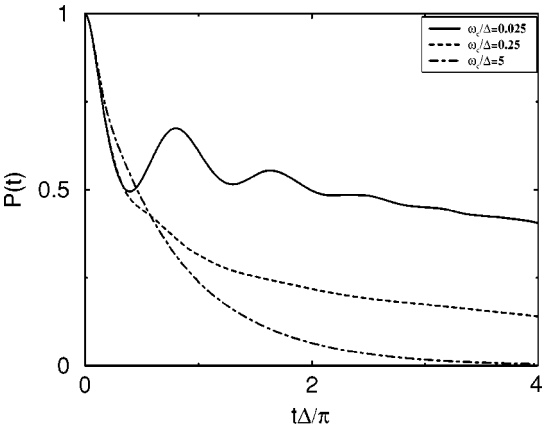

FIG. 10. Coherent to incoherent transition along the ω_c-axis for $\beta\Delta = 0.5$ and $\eta/\Delta = 5$.

C. Electron transfer rates

In this subsection we present some results for electron-transfer rates. In particular, we will compare results obtained from numerically exact or approximate dynamical approaches with commonly used rate expressions. Stationary electron-transfer rates are only well defined if the population of the donor (or acceptor) state (possibly after a short period of nonexponential dynamics) exhibits an exponential decay. As illustrated by the results in the previous section, electron-transfer dynamics is in general more complicated than a simple exponential decay. But for sufficiently high temperature and/or strong coupling to the bath the electronic population dynamics shows exponential relaxation toward the equilibrium state. In this case the electronic population dynamics can be described by the simple kinetic equations,

$$\dot{P}_1(t) = -\kappa_f P_1(t) + \kappa_b P_2(t), \tag{3.4a}$$

$$\dot{P}_2(t) = -\kappa_b P_2(t) + \kappa_f P_1(t), \tag{3.4b}$$

where κ_f and κ_b denote the forward and backward electron-transfer rates, respectively, which are related by the principle of detailed balance,

$$\kappa_b = e^{-2\epsilon\beta}\kappa_f. \tag{3.5}$$

The corresponding kinetic equation for the difference in electronic population reads

$$\dot{P}(t) = -(\kappa_f - \kappa_b) - (\kappa_f + \kappa_b)P(t). \tag{3.6}$$

In this section we will focus on systems without electronic bias ($\epsilon = 0$). In this case the forward and backward rate are the same and the electron-transfer rate can be obtained as the long-time limit of a time-dependent decay rate in the following way:

$$\kappa_f = \lim_{t\to\infty} \kappa_f(t), \tag{3.7a}$$

$$\kappa_f(t) = -\frac{1}{2}\frac{\dot{P}(t)}{P(t)}. \tag{3.7b}$$

If the definition of a rate is meaningful, the time-dependent decay rate $\kappa_f(t)$ will reach a plateau after a certain time. In contrast to the use of the approximate rate expressions discussed below, the monitoring of $\kappa_f(t)$ therefore allows one to explicitly verify whether a rate constant description is meaningful for the particular case under consideration.

A commonly used approximation for the electron-transfer rate in the nonadiabatic regime is the so-called quantum Golden Rule rate[1,86–89]

$$\kappa_f^{\mathrm{QGR}} = 2\Delta^2\,\mathrm{Re}\int_0^\infty \mathrm{d}\tau e^{2i\epsilon\tau - Q(\tau)}, \tag{3.8}$$

with $Q(\tau)$ defined in Eq. (2.11). This quantum Golden Rule rate is closely related to the kernel of the NIBA integro-differential equation (2.9). If the typical time scale of $P(t)$ is slow compared to the decay time of the kernels K_+, K_-, the NIBA equation (2.9) can be approximated by the kinetic equation (3.6) with time-dependent rates $\kappa_f(t), \kappa_b(t)$, e.g.,

$$\kappa_f^{\mathrm{NIBA}}(t) = 2\Delta^2\,\mathrm{Re}\int_0^t \mathrm{d}\tau e^{2i\epsilon\tau - Q(\tau)} \times \exp\{i(1+y_0)(Q''(t) - Q''(t-\tau))\}. \tag{3.9}$$

This so-called nonequilibrium golden rule rate was derived by Coalson and co-workers some years ago[90] (see also Ref. 91). The standard golden rule rate (3.8) is obtained from Eq. (3.9) if the long-time limit is taken and the nuclear degrees of freedom are initially in equilibrium at the donor state (i.e., $y_0 = -1$). In the high-temperature (classical) limit the integration in Eq. (3.8) can be carried out and one obtains the classical golden rule expression,[86,92]

$$\kappa_f^{\mathrm{CLGR}} = \Delta^2\sqrt{\frac{\pi\beta}{E_r}}e^{-\beta[(E_r-2\epsilon)^2/4E_r]}. \tag{3.10}$$

In the opposite (adiabatic) limit, the electron-transfer rate is primarily determined by the dynamics of the nuclear degrees of freedom on the lower adiabatic potential energy surface and can be well described by transition state theory. In this case the rate becomes independent on the electronic coupling and reads[8,73,93] (in the high-temperature limit)

$$\kappa_f^{\mathrm{TST}} = \frac{\omega_c}{4}\sqrt{\frac{\beta E_r}{\pi}}e^{-\beta[(E_r-2\epsilon)^2/4E_r]}. \tag{3.11}$$

Several approaches have been used to obtain a simple rate expression which can tune between the adiabatic and nondiabatic regime. In the classical limit Zusman,[6] and later Garg *et al.*[7] utilizing different methods, have derived the following formula:

$$\kappa_f^{\mathrm{ZUS}} = \frac{\Delta^2}{1+g}\sqrt{\frac{\pi\beta}{E_r}}e^{-\beta[(E_r-2\epsilon)^2/4E_r]}. \tag{3.12}$$

Here, g denotes the so-called ''adiabaticity parameter'' $g = 4\pi\Delta^2/E_r\omega_c$. In the adiabatic ($g \gg 1$) or nondiabatic ($g \ll 1$) regime the Zusman rate approaches the expressions (3.10) and (3.11), respectively. From the point of view of reaction rate theory, the quantum/classical Golden Rule formulas (3.8), (3.10) as well as Eq. (3.11), correspond to quantum/classical transition state theory which is a very good approximation for ''direct'' reactions. The Zusman rate, on the other hand, can to some extent account for ''recrossing'' dynamics.

More recently, methods based on imaginary time formulations as well as real time path integral approaches have been applied to derive rate expressions in the crossover regime.[94–98] In particular, Stockburger and Mak have shown[98] that the adiabaticity parameter g in general is also a function of the temperature and can deviate from the simple form (3.12).

We first consider the moderately adiabatic regime with $\Delta/\omega_c = 4$. As was discussed above, electron-transfer rates are only well-defined for sufficiently high temperature and/or strong coupling. Figure 1 demonstrates, for example, that for a temperature of $\beta\Delta = 0.5$ the definition of an electron-transfer rate is only meaningful for coupling strength $\eta \geqslant 2$. Figure 11 shows the time dependent rate (3.7b) [extracted from a GSE calculation, which in this parameter regime is a rather good approximation (cf. Fig. 1)] for two different cou-

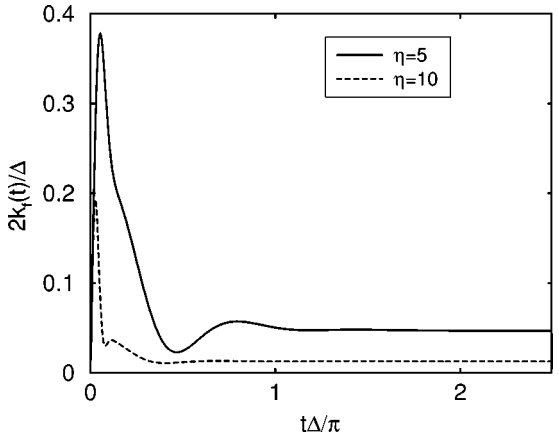

FIG. 11. Time-dependent electron transfer rate in the adiabatic regime ($\Delta/\omega_c=4$) obtained from the GSE for $\beta\Delta=0.5$: $\eta/\Delta=5$ (full line); $\eta/\Delta=10$ (dashed line).

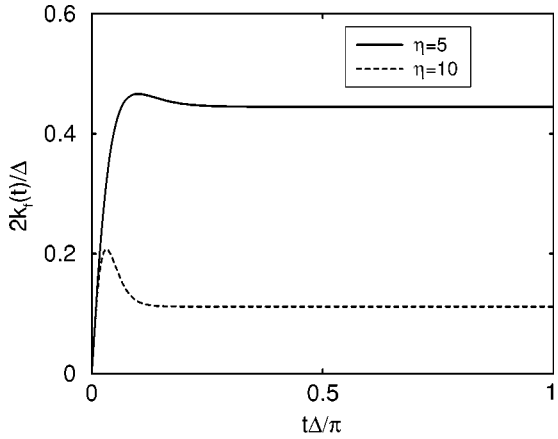

FIG. 13. Time-dependent electron transfer rate in the nonadiabatic regime ($\Delta/\omega_c=0.2$) obtained from NIBA for $\beta\Delta=0.5$: $\eta/\Delta=5$ (full line); $\eta/\Delta=10$ (dashed line).

pling strengths. It is seen that after a period of transient, nonexponential dynamics (the details of which depend on the initial state) the time dependent rate reaches a plateau which corresponds to the electron-transfer rate. [It should be noted that for smaller coupling ($2<\eta<5$) this rate describes only the slow long-time decay of the population of the donor state.] Figure 12 displays electron-transfer rates obtained from the GSE, quantum and classical Golden Rule rates, as well as the Zusman rate as a function of the coupling strength. Also shown are some results obtained with the hybrid approach. The GSE and the simulation results are in rather good agreement for small to moderate coupling strength. For very strong coupling the GSE tends to underestimate the electron-transfer rate. As to be expected, the Golden Rule formulas cannot describe the electron-transfer rate in this regime. In fact (for not too strong coupling), these rates are closer to the maximum of the time-dependent rate (3.7b) (cf. Fig. 11), confirming the transition-state theory nature of these formulas. Because of the strong recrossing dynamics (the difference between the maximum and the plateau value of the rate is about an order of magnitude for $\eta/\Delta=10$) this is a poor approximation in the present case. The Zusman rate is overall in good agreement with the GSE and the simulation results. For stronger coupling the Zusman rate shows a significant deviation from the GSE rate. Since the Zusman rate can be derived as an approximation to the smallest real eigenvalue of the GSE (see, for example, Ref. 7), this deviation signals a breakdown of the Zusman rate description and the seemingly better agreement with the rate from the simulation can only be fortuitous.

Finally, we consider an example in the nonadiabatic regime with $\omega_c/\Delta=5$. In this case the study of the population dynamics (cf. Fig. 2) shows that NIBA is an excellent approximation and, therefore, rates obtained from NIBA will be used for comparison. At a temperature of $\beta\Delta=0.5$ a coupling strength of approximately $\eta/\Delta>3$ is necessary to have a meaningful electron-transfer rate. Figure 13 displays the time dependent rate for two different coupling strengths. In contrast to the adiabatic case, here the characteristic time scale of the bath is faster than the electronic (tunneling) time and, therefore, the stationary rate plateau is reached much faster and there is very little recrossing dynamics. Figure 14

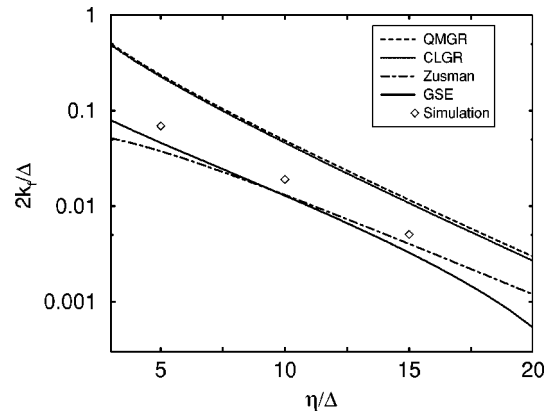

FIG. 12. Electron transfer rate in the adiabatic regime ($\Delta/\omega_c=4$) for $\beta\Delta=0.5$ as a function of the coupling strength to the bath. Shown are results from the hybrid approach simulation (diamonds), GSE (full line), quantum Golden Rule (dashed line), classical Golden Rule (dotted line), Zusman rate (dashed–dotted line).

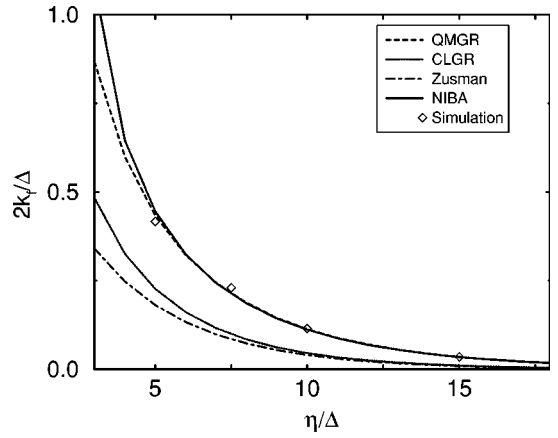

FIG. 14. Electron transfer rate in the nonadiabatic regime ($\Delta/\omega_c=0.2$) for $\beta\Delta=0.5$ as a function of the coupling strength to the bath. Shown are results from the hybrid approach simulation (diamonds), NIBA (full line), quantum Golden Rule (dashed line), classical Golden Rule (dotted line), Zusman rate (dashed–dotted line).

compares rates obtained from NIBA with quantum/classical Golden Rule rates as well as Zusman rates. It is seen that (except for small coupling) there is excellent agreement between the NIBA result and the quantum Golden Rule rate. Because of the rather low temperature, however, the classical Golden Rule, as well as the Zusman rate, are about a factor of 2 too small.

IV. CONCLUSION

In this work we have applied the self-consistent hybrid approach proposed in paper I to a spin-boson model with Debye spectral density which describes electron-transfer processes in a Debye solvent. With the hybrid approach it was possible to study this system in essentially all the parameter regimes in a numerically exact and reasonably efficient manner. In particular, we have studied the characteristics of the population dynamics in the adiabatic, nonadiabatic, and intermediate regime, as well as the coherent to incoherent transition along the three different parameter axes.

Furthermore, using the results of the hybrid approach as a benchmark, we have tested several approximate methods which have been widely used to describe the dynamics of the spin-boson model. The results of these tests can be summarized as follows: If the temperature is not too low, NIBA is found to give good results in the nonadiabatic ($\Delta/\omega_c \ll 1$), unbiased ($\epsilon=0$) regime for a broad range of electron–phonon coupling. As the temperature is lowered, NIBA may deviate from the simulation results to some extent for large electron–phonon coupling strengths, but can still provide qualitative answers. However, as for the spin-boson model with Ohmic spectral density (with exponential cutoff),[1,2] it yields qualitatively incorrect results for systems with a sizable electronic energy bias. Also, our results show that NIBA cannot be used in the intermediate ($\Delta \approx \omega_c$) and adiabatic ($\Delta > \omega_c$) regimes (except for very weak coupling to the bath). This latter conclusion also applies to the Markovian and non-Markovian BRE. This (BRE) approach is in general a good approximation in the nonadiabatic, weak-coupling regime. Different from NIBA, however, it is also applicable to systems with an electronic energy bias (and weak electron–phonon coupling). In cases where ω_c/Δ is not too large we have found that the non-Markovian variant of BRE is somewhat better than the Markovian BRE, although the difference is quite small.

The results of the GSE (Zusman equation) were found to be generally in good agreement with the numerically exact results in the high temperature regime ($\beta\omega_c < 1$). In contrast to the BRE, this (GSE) approach can therefore be applied to strong electron–phonon coupling regimes as long as the temperature is high enough. Moreover, our results also show that in contrast to the NIBA the validity of the GSE approach is not restricted to the nonadiabatic regime. The classical Ehrenfest model, with only two electronic states treated quantum mechanically, is in general a good approximation for adiabatic regimes where the GSE is applicable. However, for strong electron–phonon coupling cases, it can deviate significantly from the true quantum mechanical results even for a reasonably high temperature, whereas the GSE can still provide a quantitative description. This is presumably due to the quantum interference effects between the electronic states and the ''reaction coordinate,'' which is included to some extent in the GSE but missing from the classical Ehrenfest model. A better approximation would be to use the same strategy as in the GSE, i.e., to form a composite quantum subsystem by including the two electronic states as well as the reaction coordinate, and treat the remaining bath modes classically. Such a strategy will also likely improve the efficiency of our self-consistent hybrid approach: one expects the most important quantum effects to be captured by the interaction of electronic states with the reaction coordinate, and thus may require putting a smaller percentage of other modes into the quantum core.

The overall comparisons also show that there are at least two regimes where none of the tested approximate methods give reliable results: the intermediate ($\Delta \approx \omega_c$), strong-coupling regime and the moderately adiabatic ($0.2 < \omega_c/\Delta < 1$), low-temperature, strong-coupling regime. This is an important parameter range, for example, for electron-transfer reactions in mixed-valence compounds.

The spin-boson model investigated in this paper includes only two electronic energy levels, describing the donor and acceptor state, respectively. To model long-distance electron-transfer reactions in bridged systems (such as, for example, electron transfer in photosynthetic reaction centers or in DNA) more electronic states must be taken into account to describe the dynamics correctly. As the application to the electronic resonance system in paper I demonstrates, the hybrid approach is well suited to study these types of problems.

In the present study of a solvent exhibiting Debye electronic relaxation the reaction coordinate is overdamped and, therefore, all coherent features in the dynamics are of electronic origin. In systems with an underdamped reaction coordinate (or combinations of different reaction modes), describing, for example, high frequency vibrations in intramolecular electron-transfer reactions, vibrational coherence may also be of importance.[68,81–85] Of particular interest is the question of observability and quenching of this vibrational coherent motion if the system is interacting with its environment (as is the case, for example, in intramolecular electron-transfer processes in large molecules or proteins). Work in this direction is in progress.

ACKNOWLEDGMENTS

This work was supported by the Director, Office of Science, Office of Basic Energy Sciences, Chemical Sciences Division of the U. S. Department of Energy under Contract No. DE-AC03-76SF00098, and by the National Science Foundation Grant No. CHE 97-32758. One of the authors (M.T.) gratefully acknowledges a Feodor-Lynen fellowship of the Alexander von Humboldt Foundation and thanks W. Domcke, D. Egorova, A. Lucke, and I. Goychuk for helpful discussions.

[1] U. Weiss, *Quantum Dissipative Systems* (World Scientific, Singapore, 1993).
[2] A. J. Leggett, S. Chakravarty, A. T. Dorsey, M. P. A. Fisher, A. Garg, and W. Zwerger, Rev. Mod. Phys. **59**, 1 (1987).
[3] H. Wipf, D. Steinbinder, K. Neumaier, P. Gutsmiedl, A. Magerl, and A. Dianoux, Europhys. Lett. **4**, 1379 (1987).
[4] A. Suarez and R. Silbey, J. Chem. Phys. **94**, 4809 (1991).

[5] U. Weiss, H. Grabert, and S. Linkwitz, J. Low Temp. Phys. **68**, 213 (1987).
[6] L. Zusman, Chem. Phys. **49**, 295 (1980).
[7] A. Garg, J. Onuchic, and V. Ambegaokar, J. Chem. Phys. **83**, 4491 (1985).
[8] I. Rips and J. Jortner, J. Chem. Phys. **87**, 2090 (1987).
[9] C. Aslangul, N. Pottier, and D. Saint-James, J. Phys. (Paris) **47**, 1657 (1986).
[10] R. D. Coalson, J. Chem. Phys. **86**, 995 (1987).
[11] R. Göhrlich, M. Sassetti, and U. Weiss, Europhys. Lett. **10**, 507 (1989).
[12] D. Y. Yang and R. I. Cukier, J. Chem. Phys. **91**, 281 (1989).
[13] M. Sassetti and U. Weiss, Phys. Rev. A **41**, 5383 (1990).
[14] C. H. Mak and D. Chandler, Phys. Rev. A **44**, 2352 (1991).
[15] R. Egger and U. Weiss, Z. Phys. B: Condens. Matter **89**, 97 (1992).
[16] R. Egger and C. H. Mak, Phys. Rev. B **50**, 15210 (1994).
[17] N. Makri and D. E. Makarov, J. Chem. Phys. **102**, 4600 (1995).
[18] D. E. Makarov and N. Makri, Chem. Phys. Lett. **221**, 482 (1994).
[19] G. Stock, J. Chem. Phys. **103**, 1561 (1995).
[20] G. Stock, Phys. Rev. E **51**, 3038 (1995).
[21] M. Winterstetter and U. Weiss, Chem. Phys. **209**, 1 (1996).
[22] D. G. Evans and R. D. Coalson, J. Chem. Phys. **104**, 3598 (1996).
[23] A. Lucke, C. H. Mak, R. Egger, J. Ankerhold, J. Stockburger, and H. Grabert, J. Chem. Phys. **107**, 8397 (1997).
[24] J. Stockburger and C. H. Mak, Phys. Rev. Lett. **80**, 2657 (1998).
[25] X. Sun, H. Wang, and W. H. Miller, J. Chem. Phys. **109**, 7064 (1998).
[26] H. Wang, X. Song, D. Chandler, and W. H. Miller, J. Chem. Phys. **110**, 4828 (1999).
[27] Y. Jung, R. J. Silbey, and J. Cao, J. Phys. Chem. A **103**, 9460 (1999).
[28] A. A. Golosov, R. A. Friesner, and P. Pechukas, J. Chem. Phys. **110**, 138 (1999).
[29] G. Stock and U. Müller, J. Chem. Phys. **111**, 65 (1999).
[30] M. Grifoni, E. Paladino, and U. Weiss, Eur. Phys. J. B **10**, 719 (1999).
[31] A. A. Golosov, R. A. Friesner, and P. Pechukas, J. Chem. Phys. **112**, 2095 (2000).
[32] H. Wang, J. Chem. Phys. **113**, 9948 (2000).
[33] R. P. Feynman and F. L. Vernon, Ann. Phys. (N.Y.) **24**, 118 (1963).
[34] R. P. Feynman and A. R. Hibbs, *Quantum Mechanics and Path Integrals* (McGraw–Hill, New York, 1995).
[35] H.-D. Meyer, U. Manthe, and L. S. Cederbaum, Chem. Phys. Lett. **165**, 73 (1990).
[36] U. Manthe, H.-D. Meyer, and L. S. Cederbaum, J. Chem. Phys. **97**, 3199 (1992).
[37] M. H. Beck, A. Jäckle, G. A. Worth, and H.-D. Meyer, Phys. Rep. **324**, 1 (2000).
[38] U. Müller and G. Stock, J. Chem. Phys. **107**, 6230 (1997).
[39] U. Müller and G. Stock, J. Chem. Phys. **111**, 77 (1999).
[40] N. F. Mott, Proc. Cambridge Philos. Soc. **27**, 553 (1931).
[41] J. B. Delos and W. R. Thorson, Phys. Rev. A **6**, 720 (1972).
[42] G. D. Billing, Chem. Phys. Lett. **30**, 391 (1975).
[43] D. A. Micha, J. Chem. Phys. **78**, 7138 (1983).
[44] R. Graham and M. Höhnerbach, Z. Phys. B: Condens. Matter **57**, 233 (1984).
[45] G. D. Billing, J. Chem. Phys. **99**, 5849 (1993).
[46] G. Stock, J. Chem. Phys. **103**, 2888 (1995).
[47] J. C. Tully and R. K. Preston, J. Chem. Phys. **55**, 562 (1971).
[48] W. H. Miller and T. F. George, J. Chem. Phys. **56**, 5637 (1972).
[49] J. C. Tully, J. Chem. Phys. **93**, 1061 (1990).
[50] M. F. Herman, J. Chem. Phys. **76**, 2949 (1982).
[51] F. J. Webster, P. J. Rossky, and R. A. Friesner, Comput. Phys. Commun. **63**, 494 (1991).
[52] S. Chapman, Adv. Chem. Phys. **82**, 423 (1992).
[53] D. F. Coker and L. Xiao, J. Chem. Phys. **102**, 496 (1995).
[54] H. Wang, M. Thoss, and W. H. Miller, J. Chem. Phys. **115**, 2979 (2001), preceding paper.
[55] G. A. Worth, H.-D. Meyer, and L. S. Cederbaum, J. Chem. Phys. **109**, 3518 (1998).
[56] A. Raab, G. A. Worth, H.-D. Meyer, and L. S. Cederbaum, J. Chem. Phys. **110**, 936 (1999).
[57] R. A. Marcus, J. Chem. Phys. **43**, 679 (1965).
[58] M. Sparpaglione and S. Mukamel, J. Chem. Phys. **88**, 3263 (1988).
[59] J. Tang, J. Chem. Phys. **104**, 9408 (1996).
[60] N. Makri and D. E. Makarov, J. Chem. Phys. **106**, 2286 (1994).
[61] R. A. Harris and R. Silbey, J. Chem. Phys. **78**, 7330 (1983).
[62] C. Meier and D. J. Tannor, J. Chem. Phys. **111**, 3365 (1999).
[63] L. Hartmann, I. Goychuk, M. Grifoni, and P. Hänggi, Phys. Rev. E **61**, 4687 (2000).
[64] J. M. Jean and R. A. F. G. R. Fleming, J. Chem. Phys. **96**, 5827 (1992).
[65] V. May, O. Kühn, and M. Schreiber, J. Phys. Chem. **97**, 12591 (1993).
[66] W. T. Pollard and R. A. Friesner, J. Chem. Phys. **100**, 5054 (1994).
[67] B. Wolfseder and W. Domcke, Chem. Phys. Lett. **259**, 113 (1996).
[68] B. Wolfseder, L. Seidner, G. Stock, W. Domcke, M. Seel, S. Engleitner, and W. Zinth, Chem. Phys. **233**, 323 (1998).
[69] A. J. Leggett, Phys. Rev. B **30**, 1208 (1984).
[70] Strictly speaking, the derivation of the Master equation (2.26) assumes an initial state which factorizes into an arbitrary initial state for the reaction coordinate and the thermal state for the remaining bath modes instead of the ''correlated'' equilibrium state ρ_B. But the effect of this difference in the initial state of the bath on the electronic population dynamics is negligible in the high-temperature regime.
[71] A. O. Caldeira and A. J. Leggett, Physica A **121**, 587 (1983).
[72] C. W. Gardiner, *Handbook of Stochastic Methods* (Springer, Berlin, 1983).
[73] L. Hartmann, I. Goychuk, and P. Hänggi, J. Chem. Phys. **113**, 11159 (2000).
[74] C. Creutz, Prog. Inorg. Chem. **30**, 1 (1993).
[75] D. G. Evans, A. Nitzan, and M. A. Ratner, J. Chem. Phys. **108**, 6387 (1997).
[76] J. Cao, Chem. Phys. Lett. **312**, 606 (1999).
[77] C. C. Moser, J. M. Keske, K. Warncke, R. S. Farid, and P. L. Dutton, Nature (London) **355**, 796 (1992).
[78] B. Carmeli and D. Chandler, J. Chem. Phys. **82**, 3400 (1985).
[79] This failure of first order perturbation theory to describe decay rates in systems with a large mismatch between the system frequency and the characteristic frequency of the bath is well known from the theory of vibrational relaxation processes (Refs. 99, 100).
[80] Similar problems of the classical Ehrenfest approach for a biased spin-boson system were reported recently by Müller and Stock (Ref. 39). These authors showed that this failure of the Ehrenfest approach is related to an unphysical flow of zero-point energy.
[81] M. H. Vos, F. Rappaport, J.-C. Lambry, J. Breton, and J.-L. Martin, Nature (London) **363**, 320 (1993).
[82] D. Jonas, S. Bradford, S. Passino, and G. Fleming, J. Chem. Phys. **99**, 2954 (1995).
[83] D. C. Arnett, P. Vohringer, and N. F. Scherer, J. Am. Chem. Soc. **117**, 12262 (1195).
[84] S. Spörlein, W. Zinth, and J. Wachtveitl, J. Phys. Chem. B **102**, 7492 (1998).
[85] I. V. Rubtsov and K. Yoshihara, J. Phys. Chem. A **103**, 10202 (1999).
[86] V. G. Levich and R. R. Dogonadze, Dokl. Akad. Nauk SSSR **124**, 123 (1959).
[87] A. A. Ovchinnikov and M. Y. Ovchinnikova, Sov. Phys. JETP **29**, 688 (1969).
[88] J. Ulstrup, *Charge Transfer in Condensed Media* (Springer, Berlin, 1979).
[89] R. A. Kuharski, J. S. Bader, D. Chandler, M. Spirk, M. L. Klein, and R. W. Impey, J. Chem. Phys. **89**, 230 (1988).
[90] R. D. Coalson, D. G. Evans, and A. Nitzan, J. Chem. Phys. **101**, 436 (1994).
[91] D. G. Evans, R. D. Coalson, H. J. Kim, and Y. Dakhnovski, Phys. Rev. Lett. **75**, 3649 (1995).
[92] R. A. Marcus, Annu. Rev. Phys. Chem. **15**, 155 (1964).
[93] R. A. Marcus and N. Sutin, Biochim. Biophys. Acta **811**, 265 (1985).
[94] J. N. Gehlen and D. Chandler, J. Chem. Phys. **97**, 4958 (1992).
[95] X. Song and A. A. Stuchebrukhov, J. Chem. Phys. **99**, 969 (1993).
[96] A. A. Stuchebrukhov and X. Song, J. Chem. Phys. **101**, 9354 (1994).
[97] J. Cao, C. Minichino, and G. A. Voth, J. Chem. Phys. **103**, 1391 (1995).
[98] J. T. Stockburger and C. H. Mak, J. Chem. Phys. **105**, 8126 (1996).
[99] S. A. Egorov and J. L. Skinner, J. Chem. Phys. **103**, 1533 (1995).
[100] S. A. Egorov and B. J. Berne, J. Chem. Phys. **107**, 6050 (1997).